

ARMY RESEARCH LABORATORY



Series Solutions for Atom Guides

by William M. Golding

ARL-TR-5335

September 2010

NOTICES

Disclaimers

The findings in this report are not to be construed as an official Department of the Army position unless so designated by other authorized documents.

Citation of manufacturer's or trade names does not constitute an official endorsement or approval of the use thereof.

Destroy this report when it is no longer needed. Do not return it to the originator.

Army Research Laboratory

Adelphi, MD 20783-1197

ARL-TR-5335

September 2010

Series Solutions for Atom Guides

William M. Golding

Sensors and Electron Devices Directorate, ARL

REPORT DOCUMENTATION PAGE			Form Approved OMB No. 0704-0188		
Public reporting burden for this collection of information is estimated to average 1 hour per response, including the time for reviewing instructions, searching existing data sources, gathering and maintaining the data needed, and completing and reviewing the collection information. Send comments regarding this burden estimate or any other aspect of this collection of information, including suggestions for reducing the burden, to Department of Defense, Washington Headquarters Services, Directorate for Information Operations and Reports (0704-0188), 1215 Jefferson Davis Highway, Suite 1204, Arlington, VA 22202-4302. Respondents should be aware that notwithstanding any other provision of law, no person shall be subject to any penalty for failing to comply with a collection of information if it does not display a currently valid OMB control number. PLEASE DO NOT RETURN YOUR FORM TO THE ABOVE ADDRESS.					
1. REPORT DATE (DD-MM-YYYY) September 2010		2. REPORT TYPE Final		3. DATES COVERED (From - To) October 2009 to August 2010	
4. TITLE AND SUBTITLE Series Solutions for Atom Guides			5a. CONTRACT NUMBER		
			5b. GRANT NUMBER		
			5c. PROGRAM ELEMENT NUMBER		
6. AUTHOR(S) William M. Golding			5d. PROJECT NUMBER		
			5e. TASK NUMBER		
			5f. WORK UNIT NUMBER		
7. PERFORMING ORGANIZATION NAME(S) AND ADDRESS(ES) U.S. Army Research Laboratory ATTN: RDRL-SEE-O 2800 Powder Mill Road Adelphi MD 20783-1197			8. PERFORMING ORGANIZATION REPORT NUMBER ARL-TR-5335		
9. SPONSORING/MONITORING AGENCY NAME(S) AND ADDRESS(ES)			10. SPONSOR/MONITOR'S ACRONYM(S)		
			11. SPONSOR/MONITOR'S REPORT NUMBER(S)		
12. DISTRIBUTION/AVAILABILITY STATEMENT Approved for public release; distribution unlimited.					
13. SUPPLEMENTARY NOTES					
14. ABSTRACT In an atomic waveguide based on magnetic interactions, the forces on different spin components have opposite signs. Thus, if one component of a spinor is bound near the guiding center, another component of the spinor is repelled from the center. This is simply an example of the Stern-Gerlach effect commonly used to separate particles in different spin states. One difference is that, in the atomic guide, the spatial degrees of freedom must be quantized as well as the spin degrees of freedom. In order to accurately treat the complete quantum problem both inside and outside the guiding region, a power series solution valid for the whole real axis is developed. Thus, in principle, both the bound and unbound components of the full spinor solution can be treated within the same framework. The power series converges and can be readily summed over a large range of the radial coordinate by making use of arbitrary precision arithmetic. This technique produces high precision eigenvalues as well as detailed information about the behavior of the spinor wavefunction at both large and small distances from the origin, making it possible to perform detailed studies of atom propagation without resorting to the adiabatic approximation.					
15. SUBJECT TERMS Atomic waveguides, arbitrary precision arithmetic, atomic physics, quantum mechanics, atom interferometry, atom chips					
16. SECURITY CLASSIFICATION OF:			17. LIMITATION OF ABSTRACT UU	18. NUMBER OF PAGES 32	19a. NAME OF RESPONSIBLE PERSON William M. Golding
a. REPORT Unclassified	b. ABSTRACT Unclassified	c. THIS PAGE Unclassified			19b. TELEPHONE NUMBER (Include area code) (301) 394-1535

Contents

List of Figures	iv
List of Tables	v
1. Introduction	1
2. Development of Radial Equations	3
2.1 Hamiltonian for a Magnetic Atom	3
2.2 Eigenstates Common to H and Λ_z	5
3. Solution by the Frobenius Technique	7
3.1 Uncouple to Produce Fourth Order Differential Equations.....	7
3.2 Frobenius Series Approach	8
4. Series Evaluations Using Arbitrary Precision Arithmetic	12
4.1 Series Calculations	12
4.2 Eigenvalues: Shooting or Summing?	16
4.3 Eigenfunctions.....	19
5. Conclusions	21
6. References	22
Distribution List	23

List of Figures

Figure 1. Cross-sectional field plot of the general quadrupole guiding field used in this work. Magnetic fields come inwards along x and go outwards along y , resulting in a quadrupole null at the center that can be used for atom guiding.	4
Figure 2. Term plot of the log of the magnitude of the individual terms used in a calculation of the first series in equation 27. The target value of radius is 40 and the maximum eigenvalue is 30. The largest term in the sequence is roughly 10^{100} and therefore 120 digits needs to be used to do an adequate job of summing this series for any value of radius up to 40 for eigenvalues less than 30.	13
Figure 3. Calculation by series summation of the lowest two bound components using 15 digits of precision. This kind of result is representative of hardware floating point. Beyond a certain point the calculation breaks down. As the number of digits used in the calculation is increased, the target radius can be significantly increased. In this way, hardware floating point limits the ability to obtain accurate eigenvalues.	14
Figure 4. The same calculation as in figure 3. The only difference is that 25 digits of precision are used. One can see that the calculation can proceed to much larger target values as the number of digits is increased.	15
Figure 5. The same calculation as displayed in figures 3 and 4, except that 100 digits were used in this calculation. The effective target radius can be pushed out to 40 with very clean results. This technique lets us calculate significantly more accurate eigenvalues as well as perform checks on asymptotic series expansions for future work.	15
Figure 6. This is a blown up version of the tail of the 100-digit calculation displayed in figure 5. The plot is from radius of 0 to 40 and the scale is expanded by a factor of 10,000. Very clean damped oscillations are observed. This is an example of the power of the basic arbitrary precision techniques. In the same region where we saw complete breakdown of the calculations at 15 and 25 digits in figures 3 and 4, extremely useful information about the asymptotic behavior is obtained by simply summing the series using 100 digits of precision. This cannot be obtained directly using hardware floating point techniques.	16
Figure 7. Plot of the first 52 eigenvalues. The red points are mode type 1 eigenvalues and the blue points are mode type 2 eigenvalues; an approximate fit to the eigenvalues as a function of n is given in the text.	18
Figure 8. The first 10 type 1 mode radial eigenfunctions. The black curve with no zero crossings is the ground state wave function. The first excited state is the blue curve.	20
Figure 9. The first 10 type 2 mode radial eigenfunctions. The black curve is the lowest energy type 2 mode but is actually the first excited state of the system.	20

List of Tables

Table 1. First 52 energy eigenvalues for our system with alignment $1/2$, zero bias field and a transverse gradient of $b_1=1$. The sequence of eigenvalues alternates between type 1 and type 2 eigenvalues as n is increased. Because of this double counting the index n in the table is not the same as the index n used in the plot of figure 7.	19
--	----

INTENTIONALLY LEFT BLANK

1. Introduction

A basic type of magnetic guiding structure used on atom chips is formed by placing a long, straight current-carrying wire in an externally produced uniform magnetic field that points in a direction perpendicular to the track of the wire (Fortágh, 2007). In this configuration, the roughly circular magnetic field of the wire is cancelled along a line that parallels the wire, creating a long straight line of zero magnetic field. Cold magnetic atoms can be trapped in quantum states in this type of magnetic field minimum near to the wire and be guided along parallel to the wire direction. This forms a type of magnetic waveguide for atoms that can, in principle, be used for constructing atom interferometers and other devices based on atom guiding.

In an atomic waveguide based on magnetic interactions, the forces on different spin components have opposite signs. Thus, if one component of a spinor is bound near the guiding center, another component of the spinor is repelled from the center. This is simply an example of the Stern-Gerlach effect commonly used to separate particles in different spin states. One difference between the simple Stern-Gerlach experiment, in which only the spin degrees of freedom are quantized and the atom waveguide, is that the spatial degrees of freedom must be quantized as well as the spin in the atom guide problem.

In order to accurately treat the complete quantum problem both inside and outside the guiding region, a power series solution expanded about the guide center, yet valid for the whole real axis, has been developed. Using this series, both the bound and unbound components of the full spinor solution can be treated within the same framework. The power series converges quickly at very small radii but converges very slowly at relatively small distances from the guide center. However, this limitation is seen to be due to the fixed hardware floating point resolution available in modern computers. The power series solutions can be readily summed over a wide range of the radial coordinate by making use of software floating point techniques implemented in arbitrary precision arithmetic libraries. This technique produces high precision eigenvalues as well as detailed information about the behavior of the spinor wavefunction at both large and small distances from the origin, making it possible to perform detailed studies of atom propagation without resorting to the adiabatic approximation (Sukumar, 1997).

Numerical solutions for the quantum modes and eigenvalues of spin 1/2 and spin 1 particles in a quadrupole guide have been published elsewhere (Hinds, 2000; Potvliege, 2001; Lesanovsky, 2004; Bill, 2006); however, in all of these works, the boundary conditions used at the guide center have been chosen incorrectly and do not properly treat the regular singularity that exists there. This error in the boundary conditions clearly results from treating the two second-order radial equations (our equations 8) as though they uncouple at the origin before trying to perform a power series analysis on the full system of radial equations. The power series analysis can be performed without first decoupling the system but one must be careful not to assume that

relations like $\rho R_-(\rho) \ll R_+(\rho)$ hold as $\rho \rightarrow 0$. This type of reasoning seems to have caused problems with the boundary conditions used in these earlier works. In Blumel (1991), the Frobenius method was used on uncoupled equations to properly handle similar types of singularities in the problem of a neutron in the magnetic field of a rectilinear current, a different but related problem.

Failure to handle the boundary conditions properly leads to an incorrect description of important details of waveguide properties such as the energy spectrum and the ground state of the system. In addition, a whole class of modes goes undetected in these calculations simply because the boundary conditions are not treated carefully. The quantum properties of an atom guide cannot be treated consistently using an inconsistent basis set. Since the quantum system is linear, using incorrect boundary conditions in the numerical solution leads to apparent modes that are actually superpositions of the true modes of the system. These mixed modes cannot generally be stationary states of the system; they are mixtures of nondegenerate states. Various lifetime estimates have been performed by several authors (Hinds, 2000; Sukumar, 1997; Potvliege, 2001; Lesanovsky, 2004; Bill, 2006) using these nonstationary modes. All such estimates are questionable, since the mixed modes used for those calculations would be time dependent simply due to the normal time evolution of a conservative Hamiltonian system and this point is not made clear in those works. Thus, any time-dependent properties calculated using these nonstationary modes might actually be due to the natural unitary evolution of the conservative system and not representative of an inherent limitation of magnetic guiding. This needs to be clarified before attributing a lifetime to the states.

In a previous work (Golding, 2009), series solutions to the radial differential equations were used simply to provide accurate initial conditions appropriate for the regular singularity at the origin. However, in that work, the initial conditions were simply used to initialize various hardware precision numerical integration routines that are routinely used for solving ordinary differential equations (ODE). The shooting technique, along with a root solving approach, was used to solve for the eigenvalues of the system as well as plot the radial eigenfunctions. The differential equations solved are stiff and it is difficult to judge the accuracy of the eigenvalue results obtained using the shooting technique. This is a well known problem with the shooting technique that occurs when an exponentially growing solution is present along with an exponentially decaying solution. When the value of the decaying solution is too small, round off errors can cause the growing exponential solution to become dominant, limiting the resolution of the calculated eigenvalues. In second order systems, this problem is often handled by integrating the system in both directions and matching the two solutions in a region where both are judged to be accurate. However, in the fourth-order system studied here, there are two oscillatory solutions in addition to the two exponential solutions that contribute significantly at large distances from the center. The oscillatory solutions cause practical difficulties in establishing satisfactory boundary conditions for an inward integration of the system since one cannot simply assume that the solution simply decays to zero far from the guide center.

In this work, the solutions to the quadrupole guide problem are formulated using a power series approach. The behavior at the regular singular point is properly accounted for by using the Frobenius series method (Ince, 1956; Bender, 1978) on the fourth-order equations derived from the coupled radial spinor equations. This is, in principle, an exact answer but leaves us to solve the problem of actually summing the series. Power series generally converge slowly and they are often used only to obtain local behavior, as in our previous work. However, the power series solutions can easily be summed at large distances from the origin if arbitrary precision arithmetic is used throughout the calculation. In the computer algebra programs, Maple and Mathematica arbitrary precision arithmetic is implemented using the GNU Multiple Precision (GMP) Library (GNU, 2010). The calculations in this work were done using Maple 14. Using arbitrary precision, all of the terms in the required sums, both very big and very small, are accurately included in the calculations resulting in very accurate solutions for both the guide wave functions and eigenvalues that can be confidently used in further detailed investigations of atom guide behavior.

2. Development of Radial Equations

The equations for the radial wave functions of the quadrupole guide are derived by making use of the angular symmetry of the quadrupole magnetic field. This symmetry is expressed as the conservation of alignment, $\Lambda_z \equiv L_z - S_z$ (Hinds, 2001; Lesanovsky, 2004; Bergeman, 1989; Golding, 2009). Our approach is to find eigenfunctions that are common to both the Hamiltonian, H and the alignment Λ_z . This approach effectively separates the angular and radial dependence of the problem, leaving only a coupled system of radial equations to solve. These equations are solved exactly by series techniques and the resulting series are summed directly using arbitrary precision arithmetic.

2.1 Hamiltonian for a Magnetic Atom

The quantum description of an atom moving in a spatially dependent magnetic field must include both internal and external degrees of freedom. This means that the momentum, position, and spin degrees of freedom must all be treated as quantum operators. Using m for the mass of the atom and \vec{M} for the magnetic moment, the Hamiltonian is written as the sum of the kinetic energy, $\frac{p^2}{2m}$ and the interaction energy of the magnetic moment and the field \vec{B} . The result is

$$H = \frac{p^2}{2m} - \vec{M} \cdot \vec{B}(\vec{r}). \quad (1)$$

The magnetic field $\vec{B}(\vec{r})$ is independent of the z -direction and is taken to be an ideal quadrupole field (equation 2) extending to infinity in the x - y plane and uniform along z . An additional

uniform bias field B_0 is added in the z -direction to help control possible spin-dependent losses that may occur at the zero field point at the center of the guide. The spatial dependence of the ideal quadrupole field is given by

$$\vec{B}(\vec{r}) = B_1(-x\hat{x} + y\hat{y}) + B_0\hat{z}. \quad (2)$$

A cross-sectional plot of this field is shown in figure 1. The guiding center of this field is at the origin where the transverse field is zero. The quantity B_1 is the magnitude of the transverse field gradient. It is taken as greater than or equal to zero in this work, although changing the sign of B_1 simply changes the quadrupole field configuration from one with the field pointing inward along the x -axis to one with the field pointing inward along the y -axis.

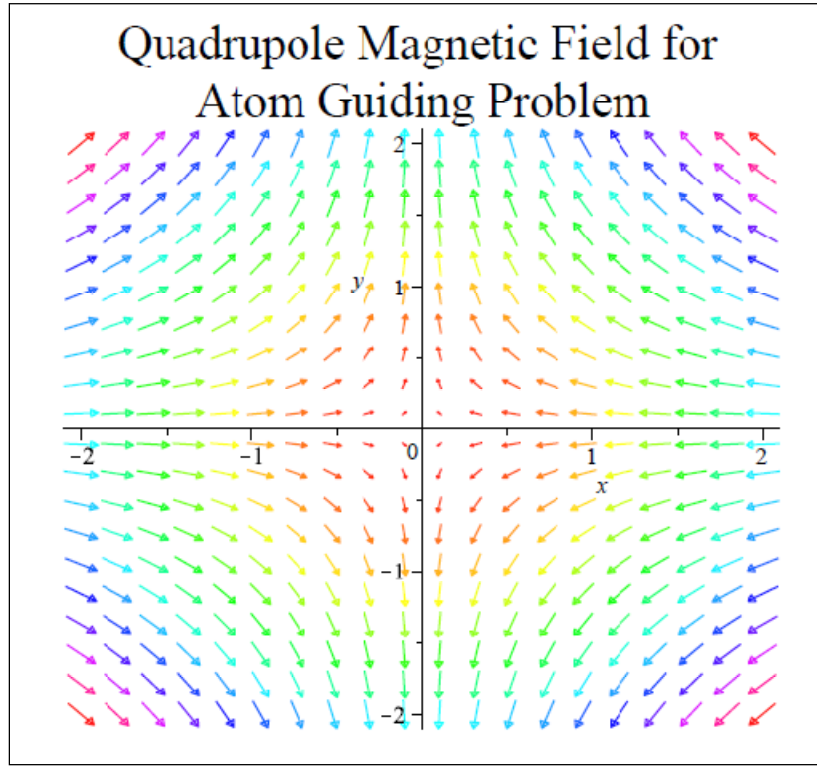


Figure 1. Cross-sectional field plot of the general quadrupole guiding field used in this work. Magnetic fields come inwards along x and go outwards along y , resulting in a quadrupole null at the center that can be used for atom guiding.

The gradient of the transverse field is what provides the trapping force that keeps the atom confined in the transverse direction. The transverse field is zero at the center of the guide and the only nonzero field component at the very center is the longitudinal bias field B_0 . The magnitude of the transverse field is $|B| = B_1\sqrt{x^2 + y^2} = B_1\rho$, where ρ is the radial coordinate in the cylindrical system. Even though the field is varying in direction as one goes round the guide, the contours of constant field magnitude are simply circles.

The potential is independent of the position along the guide. Therefore, p_z is a constant of the motion and is ignored here. In future problems, when variations in the potential along the z -direction are considered, the variations in the longitudinal momentum will be included.

Variations in the transverse potential should show up as variations in the guide propagation constant and this will affect the accuracy of sensitive measurements based on interferometry.

In the model of the atom described by equation 1, the magnetic moment of the atom is just the magnetic moment of a single outer electron. The atomic model used here can be thought of as an alkali atom with a spin zero nucleus and a total mass m . The magnetic moment is $\vec{M} = \gamma \vec{S}$, where γ is the gyromagnetic ratio of the level considered and \vec{S} is the spin angular momentum of the atom. Since a spin $\frac{1}{2}$ system is being considered, the spin angular momentum is proportional to the Pauli matrices, $\vec{S} = \frac{\hbar}{2} \vec{\sigma}$.

The Schrödinger equation for the guided atom eigenstate $\bar{\Psi}_E$ is

$$-\frac{\hbar^2}{2M} \nabla^2 \bar{\Psi}_E(\vec{r}) - \gamma \vec{S} \cdot \vec{B}(\vec{r}) \bar{\Psi}_E(\vec{r}) = E \bar{\Psi}_E(\vec{r}) \quad (3)$$

Equation 3 is made dimensionless by choosing a length scale such that $x \rightarrow \tilde{\lambda} x$, where the new x

is dimensionless. Then $\frac{\hbar^2}{2M} \nabla^2 \bar{\Psi}_E(\vec{r}) \rightarrow \frac{\hbar^2 k^2}{2M} \nabla^2 \bar{\Psi}_E(\vec{r})$ and the recoil energy is defined as

$E_R = \frac{\hbar^2 k^2}{2M}$, where $k = \frac{1}{\tilde{\lambda}}$ is the wavenumber of the optical field used to cool the atom. This is a

rather arbitrary choice at this stage, but the recoil energy is a convenient scale for atoms that have been laser cooled. After dividing through by the recoil energy, pulling out the relevant

factors, and defining the dimensionless transverse field parameter $b_1 = \gamma \frac{\hbar B_1 \tilde{\lambda}}{2E_R}$, the longitudinal

field parameter $b_0 = \gamma \frac{\hbar B_0}{2E_R}$, and the scaled energy $\varepsilon = \frac{E}{E_R}$.

2.2 Eigenstates Common to H and Λ_z

The common eigenstates of H and Λ_z are found using the eigenstates of L_z, S_z in the following way

$$\begin{aligned} H |\mu, \varepsilon\rangle &= \varepsilon |\mu, \varepsilon\rangle \\ \Lambda_z |\mu, \varepsilon\rangle &= \mu |\mu, \varepsilon\rangle. \end{aligned} \quad (4)$$

When the longitudinal bias field, b_0 is zero the Hamiltonian is invariant under various symmetry operations. This symmetry is the cause of a degeneracy of the eigenstates at $b_0 = 0$. The two

degenerate states for each value of energy have opposite alignment. The operation $P_y \sigma_x$ takes an eigenstate $|\mu, \varepsilon\rangle$ to its degenerate partner $|\mu, -\varepsilon\rangle$,

$$P_y \sigma_x |\mu, \varepsilon\rangle = |\mu, -\varepsilon\rangle, \quad (5)$$

where P_y takes y to $-y$ and σ_x exchanges the spinor components when working in the position representation. In this representation, the spinor eigenfunction is given by $\bar{\Psi}_{\mu\varepsilon}(\vec{r}) = \langle \vec{r} | \mu, \varepsilon \rangle$.

The component form is

$$\bar{\Psi}_{\mu\varepsilon}(\vec{r}) \equiv \begin{pmatrix} \psi_{+\mu\varepsilon}(\rho, \varphi) \\ \psi_{-\mu\varepsilon}(\rho, \varphi) \end{pmatrix} = e^{i\mu\varphi} \begin{pmatrix} R_{+\mu\varepsilon}(\rho) e^{i\varphi/2} \\ R_{-\mu\varepsilon}(\rho) e^{-i\varphi/2} \end{pmatrix} \quad (6)$$

and the degenerate partner is found as follows

$$\begin{aligned} P_y \sigma_x \bar{\Psi}_{\mu\varepsilon}(\vec{r}) &= P_y \sigma_x e^{i\mu\varphi} \begin{pmatrix} R_{+\mu\varepsilon}(\rho) e^{i\varphi/2} \\ R_{-\mu\varepsilon}(\rho) e^{-i\varphi/2} \end{pmatrix} \\ &= e^{-i\mu\varphi} \begin{pmatrix} R_{-\mu\varepsilon}(\rho) e^{i\varphi/2} \\ R_{+\mu\varepsilon}(\rho) e^{-i\varphi/2} \end{pmatrix} \\ &= \bar{\Psi}_{(-\mu)\varepsilon}(\vec{r}) \end{aligned} \quad (7)$$

Once the eigenstate is found for positive alignment, the degenerate partner of negative alignment is easily constructed. For this reason, positive alignment is assumed throughout the calculations when b_0 is zero and degeneracy is not an issue.

When the assumed form (equation 6) is used in the Schrödinger equation (equation 3) the angular dependence drops out leaving only the following radial equations for the specific alignment μ ,

$$\begin{aligned} L_+ R_+ &= \partial_\rho^2 R_+ + \frac{1}{\rho} \partial_\rho R_+ - \frac{(\mu+1/2)^2}{\rho^2} R_+ + (\varepsilon + b_0) R_+ = b_1 \rho R_-, \\ L_- R_- &= \partial_\rho^2 R_- + \frac{1}{\rho} \partial_\rho R_- - \frac{(\mu-1/2)^2}{\rho^2} R_- + (\varepsilon - b_0) R_- = b_1 \rho R_+. \end{aligned} \quad (8)$$

These two equations define the differential operators L_+ and L_- that will be used in section 3. In the case of a spin half particle with integral orbital angular momentum, the pair must be solved for the allowed half-integral values of the alignment $\mu = \pm \frac{1}{2}, \pm \frac{3}{2}, \pm \frac{5}{2}, \dots$, although the solutions for negative alignment are simply derived using symmetry when the bias field, b_0 is zero.

3. Solution by the Frobenius Technique

The series solution of differential equations near singular points requires the use of the Frobenius method (Ince, 1956; Bender, 1978). This is essentially a generalized power series approach that allows an extra degree of freedom for proper handling of the system behavior near regular singular points. Even though the differential equation contains singularities, the Frobenius method produces some solutions that are well behaved at the singular points and some solutions that have logarithmic or other types of singular behavior that do not usually satisfy the physical requirements of a desired solution.

The differential operator form of the coupled radial equations is useful for understanding the series solution technique that follows. The operators $L_{+/-}$ defined in equation 8 are explicitly written as

$$\begin{aligned}
 L_+ &\equiv \partial_\rho^2 + \frac{1}{\rho} \partial_\rho - \frac{(\mu+1/2)^2}{\rho^2} + (\varepsilon + b_0), \\
 L_- &\equiv \partial_\rho^2 + \frac{1}{\rho} \partial_\rho - \frac{(\mu-1/2)^2}{\rho^2} + (\varepsilon - b_0).
 \end{aligned}
 \tag{9}$$

Using operator notation the coupled system is just written as the pair of differential equations

$$\begin{aligned}
 L_+ R_+ &= b_1 \rho R_-, \\
 L_- R_- &= b_1 \rho R_+.
 \end{aligned}
 \tag{10}$$

3.1 Uncouple to Produce Fourth Order Differential Equations

In order to apply the Frobenius method to this system, the equations are uncoupled producing two fourth-order equations that are central to this technique. By solving for both R_+ and R_- directly on the right-hand side in the above system (equation 10) and substituting back into the other equation, we find the pair of fourth-order differential equations

$$\begin{aligned}
 \left(L_+ \frac{1}{b_1 \rho} L_- \right) R_- &= b_1 \rho R_-, \\
 \left(L_- \frac{1}{b_1 \rho} L_+ \right) R_+ &= b_1 \rho R_+.
 \end{aligned}
 \tag{11}$$

These equations are uncoupled in the sense that only one unknown function is involved in each. Both equations are fourth order, homogeneous linear differential equations and therefore four independent solutions are required for the general solution of each. Both equations have a regular singularity at the origin and an irregular singularity at infinity. Equations of this type are called Hamburger equations (Ince, 1956).

The general solution of each equation in equation 11 is actually only the general solution for one component of the two-component spinors defined in equation 7. The other component is found by substitution back into the original system (equation 10). Thus there are two distinct ways of finding the general solution of the system (equation 10). One could either solve the first equation in equation 11 for R_- and use the second equation of equation 10 to calculate the corresponding R_+ components or use the reverse process to get R_- from R_+ . Because the Frobenius method always produces a log-free solution for the largest indicial index found, these two reversed solution processes determine the two distinct types of physically acceptable modes in this system.

3.2 Frobenius Series Approach

The Frobenius series technique is applied by assuming a modified power series solution of the form

$$R_{p1} = \sum_{n=0}^{\infty} cp_n \rho^{n+\sigma_1}, \quad (12)$$

where the coefficients cp_n and the index σ_1 are unknown except that $cp_0 = 1$. In both the subscript $p1$ and in the coefficient cp , the p refers to the fact that this solution process starts with the spin-up (or plus) radial component. The number 1 in the subscripts labels these solutions as modes of type 1. The reverse solution process will produce modes of type 2 and the letter m will indicate a spin-down or (minus) component. Setting $R_+ = R_{p1}$ in the lower equation of equation 11 results in

$$\begin{aligned} \left(L_- \frac{1}{b_1 \rho} L_+ \right) R_{p1} &= b_1 \rho R_{p1} \\ \sum_{n=0}^{\infty} cp_n \left(L_- \frac{1}{\rho} L_+ \right) \rho^{n+\sigma_1} &= b_1^2 \sum_{n=0}^{\infty} cp_n \rho^{n+\sigma_1+1} . \\ \sum_{n=0}^{\infty} \left(cp_n L_- \frac{1}{\rho} L_+ - b_1^2 cp_{n-1} \right) \rho^{n+\sigma_1} &= 0 \end{aligned} \quad (13)$$

The result of letting the operator $L_- \frac{1}{\rho} L_+$ act on $\rho^{n+\sigma_1}$ is

$$\left(L_- \frac{1}{\rho} L_+ \right) \rho^{n+\sigma_1} = \left(\frac{P_1}{\rho} + \frac{P_3(n, \sigma_1)}{\rho^3} + \frac{P_5(n, \sigma_1)}{\rho^5} \right) \rho^{n+\sigma_1} \quad (14)$$

and the functions P_i are defined here

$$\begin{aligned} P_1 &= \varepsilon^2 - b_0^2 \\ P_3(n, \sigma) &= 2\varepsilon\sigma^2 + (4\varepsilon n - 2\varepsilon - 2b_0)\sigma + 2\varepsilon n^2 + (-2b_0 - 2\varepsilon)n + \varepsilon/2 - 2\varepsilon\mu^2 + 2b_0\mu + b_0 \\ P_5(n, \sigma) &= n^4 + (4\sigma - 6)n^3 + (17/2 - 18\sigma - 2\mu^2 + 6\sigma^2)n^2 + \\ &\quad (4\sigma^3 - 18\sigma^2 + (17 - 4\mu^2)\sigma + 3/2 + 6\mu^2 + 6\mu)n + \\ &\quad \sigma^4 - 6\sigma^3 + (-2\mu^2 + 17/2)\sigma^2 + (3/2 + 6\mu^2 + 6\mu)\sigma - 9\mu + \mu^4 - 19/2\mu^2 - \frac{35}{16} \end{aligned} \quad (15)$$

Inserting equation 14 into equation 13 produces

$$\sum_{n=0}^{\infty} (cp_n P_1 \rho^{n+\sigma_1-1} + cp_n P_3(n, \sigma_1) \rho^{n+\sigma_1-3} + cp_n P_5(n, \sigma_1) \rho^{n+\sigma_1-5} - b_1^2 cp_{n-1} \rho^{n+\sigma_1}) = 0. \quad (16)$$

By adjusting the indices in the terms of equation 16, an equation in which each term of the sum contains only one power of ρ can be obtained. In this form, the coefficients cp_n are defined to be zero for negative n and it is easy to pick out both the indicial equation and the recurrence relations for the coefficients,

$$\begin{aligned} \sum_{n=0}^{\infty} (cp_n P_5(n, \sigma_1) + cp_{n-2} P_3(n-2, \sigma_1) + cp_{n-4} P_1 - b_1^2 cp_{n-6}) \rho^{n+\sigma_1-5} &= 0 \\ cp_n &= 0 \text{ for } n < 0 \\ cp_0 &= 1 \end{aligned} \quad (17)$$

This equation is solved by setting the factor multiplying $\rho^{n+\sigma_1-5}$ to zero for each n . This produces the following system of equations that defines both the indicial equations and the recurrence relations for the coefficients,

$$cp_n P_5(n, \sigma_1) + cp_{n-2} P_3(n-2, \sigma_1) + cp_{n-4} P_1 - b_1^2 cp_{n-6} = 0, \quad n = 0 \dots \infty. \quad (18)$$

The first several of these equations have been written out explicitly here,

$$\begin{aligned}
n=0, & \quad cp_0P_5(0, \sigma_1) = 0, \\
n=1, & \quad cp_1P_5(1, \sigma_1) = 0, \\
n=2, & \quad cp_2P_5(2, \sigma_1) + cp_0P_3(0, \sigma_1) = 0, \\
n=3, & \quad cp_3P_5(3, \sigma_1) + cp_1P_3(1, \sigma_1) = 0, \\
n=4, & \quad cp_4P_5(4, \sigma_1) + cp_2P_3(2, \sigma_1) + cp_0P_1 = 0, \\
n=5, & \quad cp_5P_5(5, \sigma_1) + cp_3P_3(3, \sigma_1) + cp_1P_1 = 0, \\
n=6, & \quad cp_6P_5(6, \sigma_1) + cp_4P_3(4, \sigma_1) + cp_2P_1 - b_1^2cp_0 = 0, \\
n=7, & \quad cp_7P_5(7, \sigma_1) + cp_5P_3(5, \sigma_1) + cp_3P_1 - b_1^2cp_1 = 0, \\
n=8, & \quad cp_8P_5(8, \sigma_1) + cp_6P_3(6, \sigma_1) + cp_4P_1 - b_1^2cp_2 = 0, \dots
\end{aligned} \tag{19}$$

Since $cp_0 = 1$, the $n = 0$ equation determines the allowed values of σ_1 in terms of the alignment. This is the indicial equation and is given by $P_5(0, \sigma_1) = 0$ or

$$\sigma_1^4 - 6\sigma_1^3 + (-2\mu^2 + 17/2)\sigma_1^2 + (3/2 + 6\mu^2 + 6\mu)\sigma_1 - 9\mu + \mu^4 - 19/2\mu^2 - \frac{35}{16} = 0 \tag{20}$$

By inspecting equation 19, it can be determined that all of the odd n coefficients cp_n are zero since $P_5(1, \sigma_1) \neq 0$ and all odd coefficients are proportional to cp_1 .

The roots of the indicial equation in equation 20 determine the form of the solutions for R_{p1} generated by the Frobenius technique. The four roots are

$$\sigma_1 = [\mu + 1/2, -\mu + 7/2, \mu + 5/2, -\mu - 1/2]. \tag{21}$$

The allowed values for μ are positive half-integers so all of the values of σ_1 are integers. In the Frobenius method, repeated roots and roots separated by integers generally introduce logarithmic singularities into the solutions and negative values of σ_1 produce solutions with poles at the origin. All of the singular solutions must be excluded in the physical problem. In the Frobenius method, the solution corresponding to the largest indicial root is always free of logarithmic terms. For $\mu \geq 1/2$, the largest allowed value of σ_1 is always $\mu + 5/2$.

This calculation is essentially repeated for the type 2 modes by solving the first of equation in equation 11 using

$$R_- = R_{m2} = \sum_{n=0}^{\infty} cm_n \rho^{n+\sigma_2} \tag{22}$$

to develop the slightly different indicial equation for σ_2 ,

$$\sigma_2^4 - 6\sigma_2^3 + (-2\mu^2 + 17/2)\sigma_2^2 + (3/2 + 6\mu^2 - 6\mu)\sigma_2 + 9\mu + \mu^4 - 19/2\mu^2 - \frac{35}{16} = 0. \tag{23}$$

This indicial equation can be obtained directly from equation 20 by simply changing the sign of μ and the solutions are easily obtained in the same way from equation 21,

$$\sigma_2 = [-\mu + 5/2, -1/2 + \mu, \mu + 7/2, 1/2 - \mu]. \quad (24)$$

However, the largest index for positive μ is now $\mu + 7/2$ and since the largest index is always log-free, the solution (equation 22) using this value of σ_2 is the second physically acceptable solution of the system and is referred to as mode 2.

It is straightforward to see that for $\mu > 7/2$ there are at least two solutions to equation 11 that are unacceptable because of the ρ^σ singularity at the origin. For smaller values of μ , it is not as obvious because there are some cases in which three values of σ are unique integers. In these cases, the three solutions need to be checked more carefully to be certain they are not all log-free. We have checked this using the computer algebra program, Maple, and it turns out that two, and only two, log-free modes can be found for any value of μ in this system.

Once the allowed indices have been determined, the coefficients of the series expansions equations 12 and 22 must be found to complete the solution. The cp_n are determined directly from equation 18 as

$$cp_n = \frac{-cp_{n-2}P_3(n-2, \sigma_1) - cp_{n-4}P_1 + b_1^2 cp_{n-6}}{P_5(n, \sigma_1)} \quad n \geq 2 \text{ and even} \quad (25)$$

and a similar expression is obtained by the same technique for the cm_n . The recurrence relations defining the two physically acceptable solutions, determined by $\sigma_1 = \mu + 5/2$ for the cp_n and $\sigma_2 = \mu + 7/2$ for the cm_n are

$$cp_n = \frac{b_1^2 cp_{n-6} + (b_0^2 - \varepsilon^2) cp_{n-4} - 2n(\varepsilon(2\mu + n) - b_0) cp_{n-2}}{n(n+2)(2\mu + n + 3)(2\mu + n - 1)},$$

$$cm_n = \frac{b_1^2 cm_{n-6} + (b_0^2 - \varepsilon^2) cm_{n-4} - 2(n+1+2\mu)(\varepsilon n + \varepsilon + b_0) cm_{n-2}}{n(4+n)(2\mu + n + 3)(2\mu + n + 1)}, \quad (26)$$

$$cp_0 = 1, cm_0 = 1,$$

$$cp_n = 0, cm_n = 0 \text{ for all even } n \text{ and for all } n < 0$$

Using these recurrence relations, the following power series solutions for the two types of physical modes can be used directly for calculating eigenvalues, eigenfunctions, and the quantum behavior of the quadrupole waveguide. The mode 1 solutions for both spinor components are

$$R_{p1} = \rho^{\mu+5/2} \sum_{n=0}^{\infty} cp_n \rho^n,$$

$$R_{m1} = \frac{\rho^{\mu-1/2}}{b_1} \sum_{n=0}^{\infty} cp_n \rho^n (4\mu + 2\mu n + 6 + 5n + n^2) + \frac{(\varepsilon + b_0)}{b_1} \rho^{\mu+3/2} \sum_{n=0}^{\infty} cp_n \rho^n \quad (27)$$

and the equivalent solutions for the mode 2 spinor components are

$$\begin{aligned}
 R_{m2} &= \rho^{\mu+7/2} \sum_{n=0}^{\infty} c m_n \rho^n, \\
 R_{p2} &= \frac{\rho^{\mu+1/2}}{b_1} \sum_{n=0}^{\infty} c m_n \rho^n (8\mu + 2\mu n + 12 + 57n + n^2) + \frac{(\varepsilon - b_0)}{b_1} \rho^{\mu+5/2} \sum_{n=0}^{\infty} c m_n \rho^n.
 \end{aligned} \tag{28}$$

4. Series Evaluations Using Arbitrary Precision Arithmetic

The waveguide modes are completely defined by the coefficients in equation 26 and the series solutions presented in equations 27 and 28. In order to find the eigenvalues, the series solutions are evaluated at some large value of ρ and ε is adjusted until the bound component of the spinor at that large radius is near zero. The bound component is just the combination $R_p + R_m$ (Hinds, 2000; Golding, 2009) for the specific mode type, either 1 or 2. Asymptotic analysis shows that the bound components die off exponentially, but there is a small quickly decaying oscillatory component that can have an effect on the eigenvalues calculated using this technique and this possibility must be studied further.

The series solutions converge but they cannot be easily summed using the standard floating point hardware available in most computers. The solution adopted here is to use an existing implementation of arbitrary precision arithmetic for these calculations. The computer algebra program Maple makes use of the GNU Multiple Precision (GMP) Library (GNU, 2010) to perform the basic arithmetic calculations addition, subtraction, division, multiplication, and exponentiation. These operations are all that are needed to sum the power series solutions in equations 27 and 28 to perform the calculations reported in section 4.1.

4.1 Series Calculations

The basic difficulty in direct summation of the series solutions in equations 27 and 28 is not that the series diverge or that they do not converge quickly, it is really just that the intermediate terms in the sum are very large and cannot be represented accurately in hardware floating point. Arbitrary precision arithmetic techniques eliminate this constraint at the expense of some speed and efficiency. The tradeoff is extremely useful when extreme accuracy is needed and other techniques are suspect.

In order to do these calculations effectively, the number of digits needed to represent the largest number in the sum to at least the precision needed in the final result should be estimated. In addition, the total number of terms needed for convergence at the desired accuracy needs to be known. For example, in the solution of an eigenvalue problem, the value of an eigenfunction might be required to 20 significant digits at $\rho = 40$. In order to guarantee that the sums will be accurately calculated, individual terms of the series should be calculated for a reasonable test

case and the maximum term value obtained. If the maximum value is 10^{300} and the desired precision of the zero is 10^{-20} then at least 320 digits are needed to avoid losing precision in the final sum due to a loss of precision of any single term in the series. In practice, some guard digits should be added and convergence should be checked by changing the number of digits and the number of terms used in the calculation.

Both the number of digits and the number of terms required to evaluate a particular sum accurately can be visualized by creating a term plot. This is just a plot of the log base 10 of the magnitude of the terms in the sequence to be summed. The term plot for the series defining $R\rho_1$ is shown in figure 2. The summation calculated is the first sum in equation 27. The terms plotted are just the individual $\log_{10} |cp_n \rho^n|$ for n from zero to the largest value needed. The number of digits needed for the sum is just the difference between the maximum value and the minimum value assuming the plot is terminated when the term with the desired precision is reached.

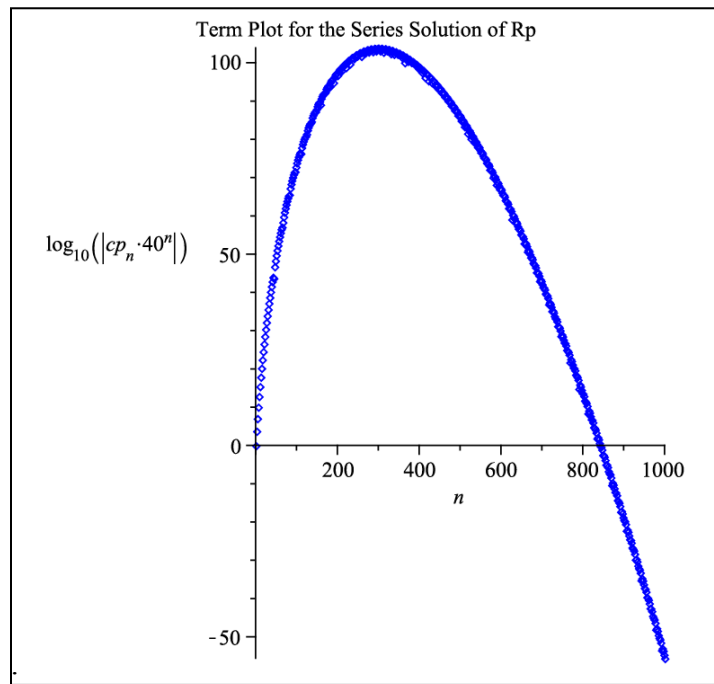


Figure 2. Term plot of the log of the magnitude of the individual terms used in a calculation of the first series in equation 27. The target value of radius is 40 and the maximum eigenvalue is 30. The largest term in the sequence is roughly 10^{100} and therefore 120 digits needs to be used to do an adequate job of summing this series for any value of radius up to 40 for eigenvalues less than 30.

If the number of required digits is underestimated, the calculation will breakdown numerically at values of the radial coordinate smaller than the desired target value. The results of using different numbers of digits in the summations are shown in figures 3, 4, and 5. In figure 3, the number of digits used is 15, which is approximately the number of digits used in floating point hardware calculations on many machines. The calculation breaks down at around $\rho = 12$. The range of the

calculation can be extended significantly by using 25 digits, as shown in figure 4. In figure 5, 100 digits were used in the calculation and there are no obvious problems with the calculations over the whole range from zero to 40. In figure 6, the tail of the 100-digit calculation is blown up by a factor of 10,000 and a very clean but heavily damped oscillation is observed. This particular oscillation can be predicted by asymptotic techniques but it has been difficult to verify in previous calculations performed at hardware precision. Understanding this behavior in detail can help avoid certain types of systematic errors in the eigenvalue calculations that involve accurately locating zeros in the tails of the eigenfunctions.

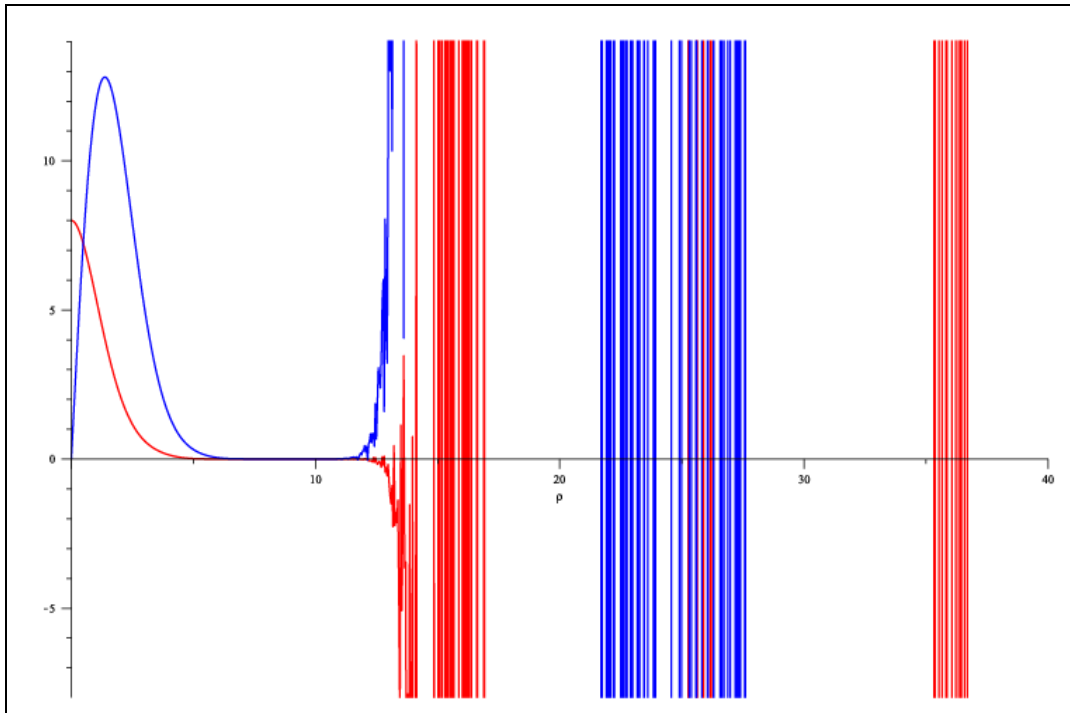


Figure 3. Calculation by series summation of the lowest two bound components using 15 digits of precision. This kind of result is representative of hardware floating point. Beyond a certain point the calculation breaks down. As the number of digits used in the calculation is increased, the target radius can be significantly increased. In this way, hardware floating point limits the ability to obtain accurate eigenvalues.

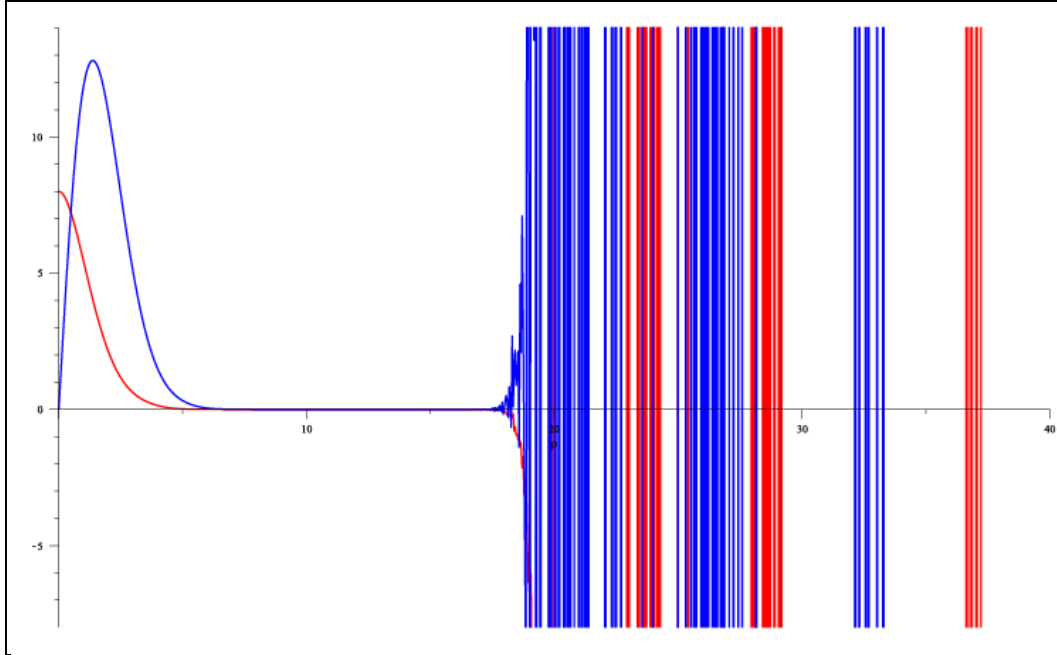


Figure 4. The same calculation as in figure 3. The only difference is that 25 digits of precision are used. One can see that the calculation can proceed to much larger target values as the number of digits is increased.

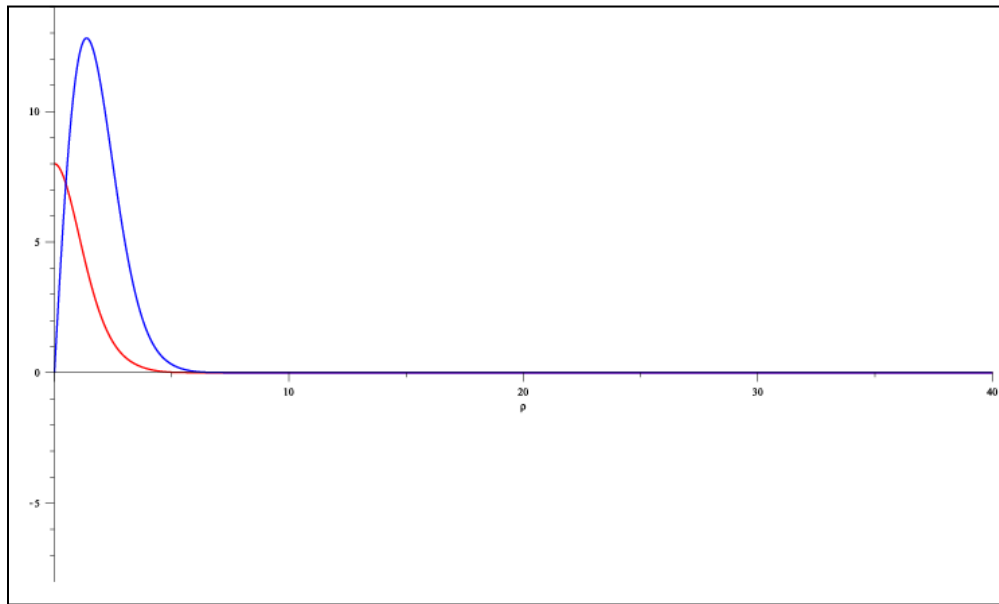


Figure 5. The same calculation as displayed in figures 3 and 4, except that 100 digits were used in this calculation. The effective target radius can be pushed out to 40 with very clean results. This technique lets us calculate significantly more accurate eigenvalues as well as perform checks on asymptotic series expansions for future work.

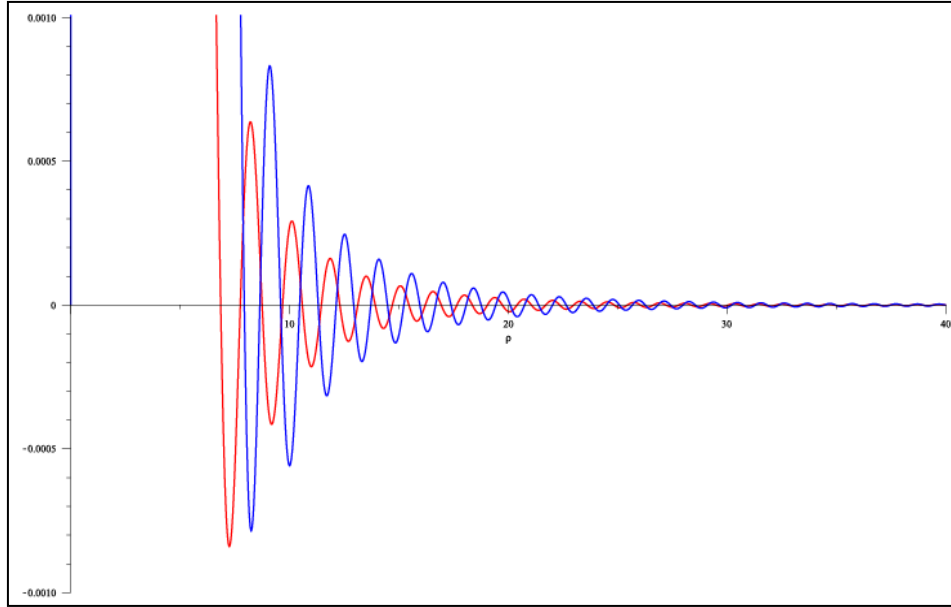


Figure 6. This is a blown up version of the tail of the 100-digit calculation displayed in figure 5. The plot is from radius of 0 to 40 and the scale is expanded by a factor of 10,000. Very clean damped oscillations are observed. This is an example of the power of the basic arbitrary precision techniques. In the same region where we saw complete breakdown of the calculations at 15 and 25 digits in figures 3 and 4, extremely useful information about the asymptotic behavior is obtained by simply summing the series using 100 digits of precision. This cannot be obtained directly using hardware floating point techniques.

4.2 Eigenvalues: Shooting or Summing?

In order to solve eigenvalue problems of the type studied here, a variation of the shooting method is used. The shooting method is the technique in which a differential equation is integrated from a boundary point where the solution is known to a target point where the solution should attain a target value. In practice, the eigenvalue or some other parameter can be adjusted so that the unknown function has the desired behavior at the target point. When the solution is acceptable, the eigenvalue or desired value of the parameter has been found. One limitation of this technique is that the differential equation solver must be able to integrate the system accurately from the known point to the target point. This can be difficult if the system is stiff or unstable or otherwise very sensitive to the exact value of the eigenvalue.

To determine the eigenvalues using the series approach, a variation of the shooting technique is used. In this approach, the solution does not depend on numerical solutions of the differential equations from an initial point to a target point. The only requirement is to accurately sum the series at the target point for various trial eigenvalues. The initial condition is built in to the series solution. The eigenvalue must be varied and the summation repeated until the target value for the unknown function is determined. This type of effective shooting technique can be accomplished over a large range of distances in systems that support arbitrary precision arithmetic and have series solutions.

Because the sum of the two components $R_p + R_m$ is an apparent bound state for both mode types 1 and 2 (Hinds, 2000; Golding, 2009), the leading behavior of this bound component dies off exponentially with distance from the center of the guide. Using this fact, the target behavior for the eigenvalue solution is just that $R_p + R_m \rightarrow 0$ as $\rho \rightarrow \infty$. The eigenvalues are then readily found using a root solving routine that uses arbitrary precision arithmetic to look for zeros of the sums defined in equations 27 and 28 at large radii. We have found that in this way the target point can be much farther from the origin than it can using the similar ODE based shooting techniques. This results in much more precise calculations of the eigenvalues. This enhanced resolution is expected to be useful as these functions are used for further calculations on the detailed properties of atom guides.

The results of eigenvalue calculations for $\mu = 1/2$, $b_0 = 0$ and $b_1 = 1$ are shown in figure 7. The first 52 eigenvalues are shown. The eigenvalue data can be approximated by the simple equation $1.893790658 + 1.270128257n^{0.7355}$. In table 1, the first 26 values of each type of mode are presented. Careful inspection shows that eigenvalues form an interleaved series in the sense that the first eigenvalue is a type 1 mode and second is a type 2 mode; this pattern holds up as far as we have checked. In figure 7, mode type 1 points are red and mode type 2 points are blue.

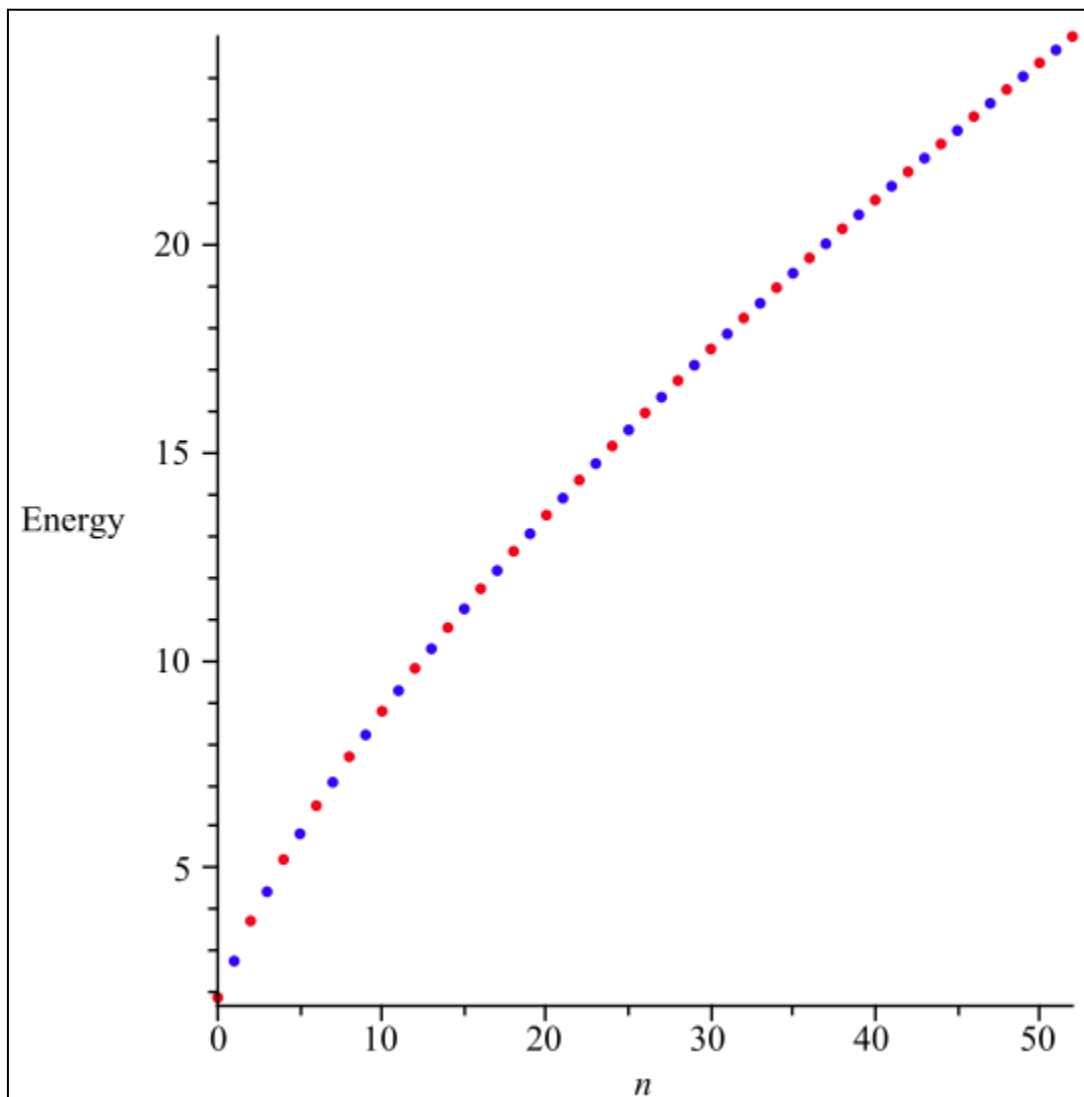


Figure 7. Plot of the first 52 eigenvalues. The red points are mode type 1 eigenvalues and the blue points are mode type 2 eigenvalues; an approximate fit to the eigenvalues as a function of n is given in the text.

Table 1. First 52 energy eigenvalues for our system with alignment 1/2, zero bias field and a transverse gradient of $b_1=1$. The sequence of eigenvalues alternates between type 1 and type 2 eigenvalues as n is increased. Because of this double counting the index n in the table is not the same as the index n used in the plot of figure 7.

n	Type 1 Eigenvalue	Type 2 Eigenvalue
1	1.893790658	2.770959115
2	3.735223647	4.436734695
3	5.211244681	5.827843267
4	6.504703191	7.067475471
5	7.681587325	8.20585412
6	8.774989674	9.269728735
7	9.80443751	10.27548299
8	10.78265521	11.23407047
9	11.71851157	12.15327128
10	12.61849734	13.03886265
11	13.48754237	13.89528345
12	14.32950179	14.72603767
13	15.14746211	15.53395267
14	15.9439429	16.32135181
15	16.72103469	17.09017376
16	17.48049623	17.84205754
17	18.22382493	18.57840462
18	18.952309	19.30042528
19	19.66706684	20.00917379
20	20.36907731	20.70557569
21	21.05920333	21.39044912
22	21.73821055	22.06452178
23	22.40678229	22.72844459
24	23.06553163	23.38280277
25	23.7150113	24.02812491
26	24.35572179	24.66489048

4.3 Eigenfunctions

Once the eigenvalues are determined, the corresponding eigenfunctions are found by a straightforward summation of the series solutions equations 27 and 28 at any desired value of ρ . The eigenfunctions determined in this way display detailed behavior in regions beyond those accessible using the hardware precision ODE shooting techniques. This type of behavior is shown in figures 8 and 9. It is clear that the bound component does not simply decay away exponentially but has a small and quickly decaying oscillatory component as well. This behavior is explained by a detailed asymptotic solution of the problem. The ability to compare the direct calculations of the series technique with the asymptotic solutions over wide ranges will be very helpful in checking various aspects of the asymptotic behavior of these solutions.

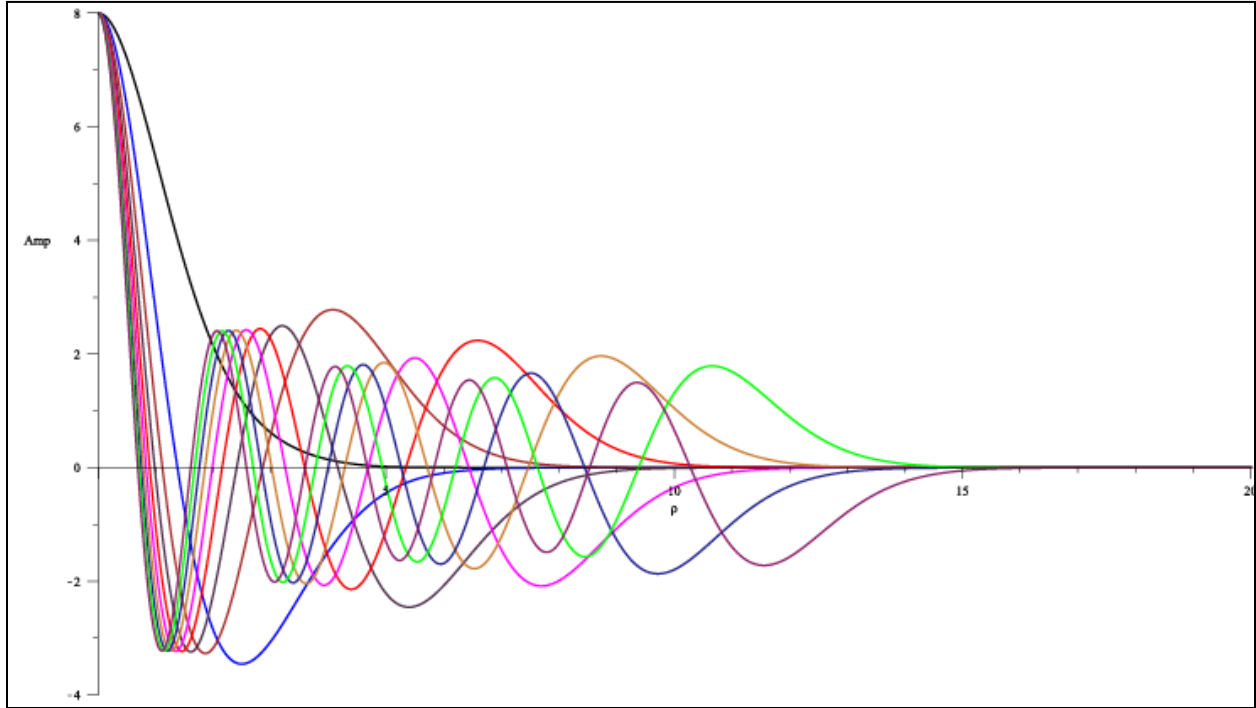


Figure 8. The first 10 type 1 mode radial eigenfunctions. The black curve with no zero crossings is the ground state wave function. The first excited state is the blue curve.

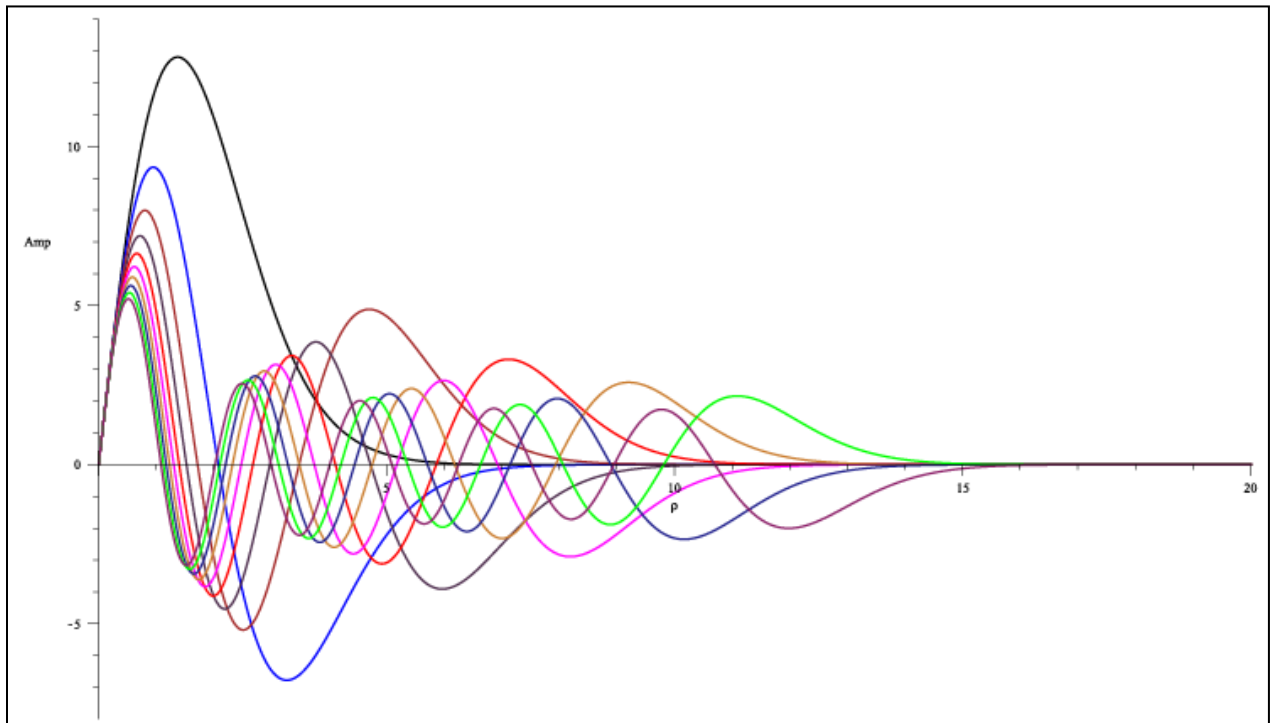


Figure 9. The first 10 type 2 mode radial eigenfunctions. The black curve is the lowest energy type 2 mode but is actually the first excited state of the system.

5. Conclusions

The use of series solution techniques along with arbitrary precision arithmetic is a very powerful combination for investigating the solutions of differential equations in regions where ordinary hardware precision numerical integration techniques break down. The use of arbitrary precision in differential equation solvers is implemented in Maple and these can be made to produce accurate solutions at large radii. However, the solution of a differential equation by the series technique simply requires the appropriate power series formulation of the solution and a software system that implements an arbitrary precision library, such as GMP (GNU, 2010). By using a judicious choice of the number of digits and terms needed for a particular set of calculations, the solutions can be calculated very quickly and with excellent resolution. We have found this technique to be extremely useful for calculating radial wavefunctions and eigenfunctions for the atomic waveguide problem as it produces accurate solutions in situations where spinor equations can be uncoupled to produce higher order differential equations that are difficult to solve analytically.

6. References

- Bender, C. M.; Orszag, S. A. *Advanced Mathematical Methods for Scientists and Engineers*; McGraw-Hill: New York, NY, 1978.
- Bergman, T. H.; et al. *JOSA B* **1989**, *6* (11), 2249.
- Bill, J. *Phys. Rev. A* **73** **2006**, 053609.
- Blümel, R.; Dietrich, K. *Phys. Rev. A* **1991**, *43*, 22–28.
- Fortágh, J.; Zimmerman, C. *RMP* **2007**, *79*, 235.
- GNU Multiprecision Library documentation located at <http://gmpilib.org/> (accessed 2010).
- Golding, W. M. *Atomic Waveguides for Atom Chips*; ARL-TR-5014; U.S. Army Research Laboratory: Adelphi, MD, Oct. 2009.
- Hinds, E. A.; Eberlein, C. *Phys. Rev. A* **2000**, *61*, 033614.
- Hinds, E. A.; Eberlein, C. *Phys. Rev. A* **2001**, *64*, 039902(E).
- Ince, E. L. *Ordinary Differential Equations*; Dover: New York, NY, 1956, p. 396.
- Lesanovsky, I.; Schmelcher, P. *Phys. Rev. A* **2004**, *70*, 063604.
- Potvliege, R. M.; Zehnlé, V. *Phys. Rev. A* **2001**, *63*, 025601.
- Sukumar, C. V.; Brink, D. M. *Phys. Rev. A* **1997**, *56*, 2451.

NO. OF COPIES	ORGANIZATION	NO. OF COPIES	ORGANIZATION
1 PDF	DEFENSE TECH INFO CTR ATTN DTIC OCA 8725 JOHN J KINGMAN RD STE 0944 FT BELVOIR VA 22060-6218	1	US GOVERNMENT PRINT OFF DEPOSITORY RECEIVING SECTION ATTN MAIL STOP IDAD J TATE 732 NORTH CAPITOL ST NW WASHINGTON DC 20402
1	DARPA ATTN J ABO-SHAEER 3701 N FAIRFAX DR ARLINGTON VA 22203-1714	1	US ARMY RSRCH LAB ATTN RDRL CIM G T LANDFRIED BLDG 4600 ABERDEEN PROVING GROUND MD 21005-5066
1 CD	OFC OF THE SECY OF DEFNS ATTN ODDRE (R&AT) THE PENTAGON WASHINGTON DC 20301-3080	1 HD 1 CD	US ARMY RSRCH OFC ATTN P REYNOLDS PO BOX 12211 RESEARCH TRIANGLE PARK NC 27709-2211
1	US ARMY RSRCH DEV AND ENGRG CMND ARMAMENT RSRCH DEV & ENGRG CTR ARMAMENT ENGRG & TECHN LGY CTR ATTN AMSRD AAR AEF T J MATTS BLDG 305 ABERDEEN PROVING GROUND MD 21005-5001	29	US ARMY RSRCH LAB ATTN IMNE ALC HRR MAIL & RECORDS MGMT ATTN RDRL CIM L TECHL LIB ATTN RDRL CIM P TECHL PUB ATTN RDRL SEE O N FELL ATTN RDRL SEE O P LEE ATTN RDRL SEE O P PELLEGRINO ATTN RDRL SEE O W M GOLDING (20 COPIES) ATTN RDRL SER E F CROWNE ATTN RDRL SES E H BRANDT ATTN RDRL SES P A EDELSTEIN ADELPHI MD 20783-1197
1	PM TIMS, PROFILER (MMS-P) AN/TMQ-52 ATTN B GRIFFIES BUILDING 563 FT MONMOUTH NJ 07703		
1	US ARMY INFO SYS ENGRG CMND ATTN AMSEL IE TD A RIVERA FT HUACHUCA AZ 85613-5300	TOTAL:	43 (40, 2 CDS, 1 PDF)
1	COMMANDER US ARMY RDECOM ATTN AMSRD AMR W C MCCORKLE 5400 FOWLER RD REDSTONE ARSENAL AL 35898-5000		
3	DEPT OF THE ARMY WEAPONS SCIENCES DIRECTORATE ATTN AMSRD AMS WS ATTN AMSRD AMS WS H EVERITT ATTN AMSRD AMS WS K MYNENI ATTN AMSRD AMS WS T BAHDER REDSTONE ARSENAL AL 35898-5000		

INTENTIONALLY LEFT BLANK